

Design options for polar-direct-drive targets from alpha heating to ignition

T J B Collins^{1,3}, J A Marozas¹, S Skupsky¹, D Cao¹, P W McKenty¹, J A Delettrez¹ and G Moses²

²University of Wisconsin,
Madison, WI 53706-1140 USA

¹Laboratory for Laser Energetics, University of Rochester,
250 East River Road, Rochester, NY 14623-1299 USA

tcol@lle.rochester.edu

Abstract. Polar direct drive (PDD) makes it possible to perform direct-drive-ignition experiments at the National Ignition Facility while the facility is configured for x-ray drive. We present the first PDD ignition-relevant target designs to include the physical effects of cross-beam energy transfer (CBET) and nonlocal heat transport, both of which substantially affect the target drive. In the PDD configuration, a multiwavelength detuning strategy was found to be effective in mitigating the loss of coupling caused by CBET, allowing for implosion speeds comparable to those of previous designs. Two designs are described: a high-adiabat alpha-burning design and a lower-adiabat ignition design.

1. Introduction

In direct-drive inertial confinement fusion, laser ablation is used to implode a spherical shell composed largely of fuel (DT), producing a central volume of high density and ion temperature. The ions, briefly confined, undergo fusion reactions, producing alpha particles, some of which are stopped in the surrounding colder, denser shell. Ignition occurs when these deposit enough energy to launch a self-sustaining thermonuclear burn wave, which consumes a fraction of the fuel before the high pressure generated by the burn wave causes the target to disassemble. Ignition occurs only if the hot-spot ion temperatures are higher than ~ 10 keV and hot-spot areal density exceeds ~ 300 mg/cm². This process is prevented if either the imploding kinetic energy is insufficient or hydrodynamic instability prevents the required hot-spot temperature and areal density.

The hot-spot volume is reduced by perturbations on the inner edge of the shell that grow as a result of the Rayleigh–Taylor instability as the shell is being decelerated by the pressure of the gas interior to it. In its current configuration, the laser beam ports of the National Ignition Facility (NIF) [1] are preferentially located away from the equator of the target sphere, for use with x-ray-driven targets enclosed in a hohlraum. Polar-direct-drive (PDD) [2,3] implosions using this configuration must contend with low-mode perturbations caused by the lack of equatorial beams. Furthermore, direct-drive experiments on the NIF [4] have demonstrated that it is necessary to model both cross-beam

³ Author to whom any correspondence should be addressed.



energy transfer (CBET) and nonlocal electron heat transport [5]. (CBET is a laser–plasma instability in which an incoming laser ray interacts with an outgoing ray by means of an intermediate ion-acoustic wave, depleting the energy of the incoming ray.) While nonlocal electron transport can increase the hydrodynamic efficiency of the implosion, CBET causes a sizable fraction of the incident laser energy to be scattered away, reducing the ablation pressure.

In this paper, we present a PDD-ignition design that addresses the two requirements given above, of shell kinetic energy and implosion uniformity, and is the first ignition design to include the effects of nonlocal heat transport and CBET. Previous ignition designs incorporated these processes in only an approximate way by using an *ad hoc* flux limiter applied to the classical expression for heat conduction. In this design, the loss of drive related to CBET is mitigated by the use of different laser wavelengths by different beams [6]. As with previous PDD designs, the drive asymmetries caused by the asymmetric disposition of the beams are controlled through a combination of individual cone pulse shapes and beam repointing. The resulting design achieves high gain for a moderate in-flight aspect ratio (IFAR). The second design we present does not ignite but has a lower IFAR for greater stability and is predicted to generate bootstrap heating producing over 10^{17} neutrons in a simulation incorporating only drive perturbations caused by beam geometry.

Section 2 describes the detuning configuration strategies. Section 3 presents the two target designs (ignition and alpha burning), followed by the conclusions in section 4.

2. Cross-Beam Energy Transfer and Wavelength Detuning

For direct-drive targets of sufficient density scale length and laser intensity, the stimulated Brillouin scattering (SBS) process is dynamically important. This process entails the parametric coupling of incident light with an ion-acoustic wave and a backscattered electromagnetic wave. The efficiency of energy transfer is determined by a resonance function of the parameter $\eta = [(\omega_i - \omega_o) - \mathbf{k}_a \cdot \mathbf{v}] / (c_a k_a)$, where ω_o and ω_i are the outgoing and incoming ray frequencies, respectively; c_a is the outflow sound speed; $\mathbf{k}_a = \mathbf{k}_o - \mathbf{k}_i$ is the ion-acoustic wave number; \mathbf{v} is the outflow velocity; and $\eta > 0$ corresponds to energy transfer from the incoming ray to the outgoing ray [7]. CBET is well known in indirect-drive inertial confinement fusion (ICF), where it is used to transfer energy between cones of beams to affect low-mode capsule symmetry. In direct-drive ICF, it is more typical for an incoming low-energy ray from the edge of a beam to rob energy from an incoming ray in the central, higher-energy portion of another beam. The energy exchange caused by CBET is determined by an attenuation factor $d\tau$, which is proportional to the resonance function $P(\eta) = \eta \cdot v_a [(\eta v_a)^2 + (1 - \eta^2)^2]^{-1}$, where v_a is the dimensionless ion-wave damping coefficient. SBS is particularly effective at robbing energy from the incoming rays because the matching condition is met over a potentially large volume near the surface where the expanding Mach number is unity. In PDD, this resonance region occurs preferentially over the equator where equatorial beams from each hemisphere overlap and where laser intensities, increased to offset the increased equatorial deposition radii, are the greatest.

CBET is mitigated in the present work by the use of wavelength detuning [6]. In this approach, the laser cavities are detuned slightly for different collections of beams to increase the frequency separation, which in turn alters the region over which the CBET efficiency is greatest. If the outgoing rays are blue shifted relative to the incoming rays, the resonance region moves to greater Mach numbers and correspondingly larger radii, where the beam overlap and corresponding energy transfer are reduced. If these rays are red shifted, the resonance region moves radially inward, and if the shift is large enough, the resonance region may, for a portion of the pulse, be hidden within the parabolic locus of turning points within which the laser rays cannot penetrate. Over time, for red-shifted outgoing rays, this resonance region moves radially outward, reducing or eliminating the CBET mitigation.

Several detuning configurations were investigated. The laser absorption efficiency for four of these configurations is shown in figure 1. The hemispherical scheme detunes the beams by hemisphere. This scheme greatly reduces the energy loss caused by the beams interacting across the equator, which is where the greatest scattering occurs. This scheme does not reduce, however, losses caused by interactions between beams from the same hemisphere. The beams on the NIF may be divided into four cones for each hemisphere: two inner cones nearer the pole and two outer cones nearer the equator. The banded scheme reverses the sign of the detuning for the two inner cones of beams in each hemisphere, increasing the coupling. The tricolor configuration improves on both of these by not

detuning the inner cones, recovering over half of the drive lost to CBET. The tricolor scheme is more effective than banded because the inner cones interact with both the equatorial beams in the same hemisphere and with the equatorial beams in the opposite hemisphere; by not detuning the inner cones, more energy is returned from the interaction across the equator than is lost to the intrahemispherical interaction. Figure 1(a) also shows the primary effect of nonlocal heat transport, an increase of hydrodynamic efficiency, especially near the equator, where the radial thermal gradient is greater. A comparison between the red and purple curves, representing implosions with and without nonlocal heat transport, shows an increase of $\sim 30\%$ in the absorbed laser energy, resulting in a much higher implosion speed. The effects of nonlocal heat transport on shock speeds have been measured experimentally [8].

All three of these schemes introduce a north–south asymmetry, as described above. This asymmetry is greatly reduced by use of a fourth configuration, balanced tri-color, in which the tricolor scheme is north to south in alternating quadrants. Figure 2(b) shows a projection in which color indicates the components of the three wavelengths. This projection plot shows a large purple region around the equator where red- and blue-shifted light overlaps, corresponding to effective CBET mitigation.

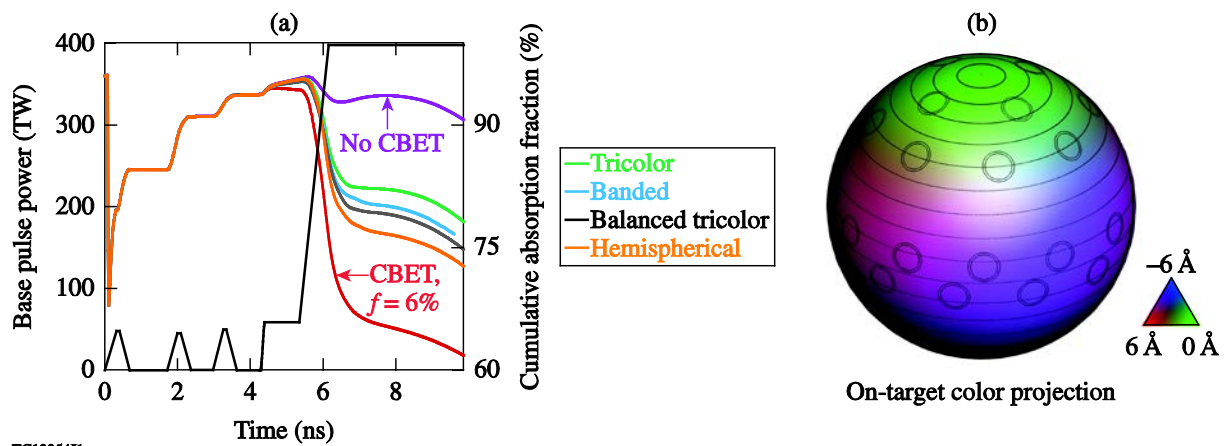
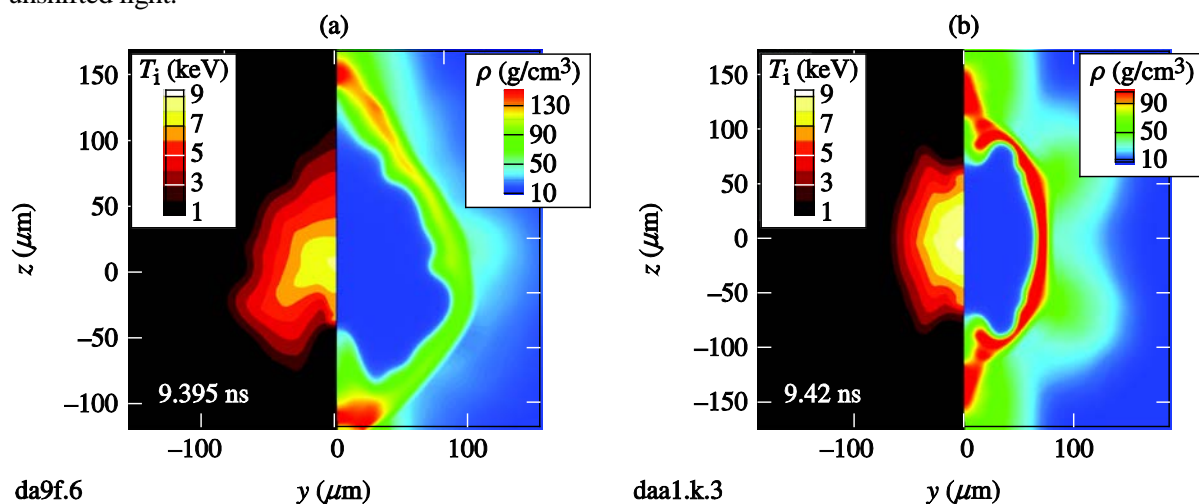


Figure 1. (a) Absorption efficiency is shown as functions of time for four detuning configurations for a PDD design tailored to achieve high gain and minimal hot-spot asymmetry when modeling nonlocal heat transport but without cross-beam energy transfer (CBET). The no-CBET case and the flux-limited CBET case are shown for comparison. (b) The projection on a surrogate target surface of the red-, blue-, and unshifted light.



da9f.6

daa1.k.3

TC12619J1

Figure 2. (a) The alpha-burning and (b) ignition designs are shown near peak compression. On the left of each contour plot is the ion temperature and on the right is the mass density.

3. Ignition and Alpha-Burning Designs Incorporating CBET and Nonlocal Heat Transport

The two designs shown here use a DT shell with a CH ablator. The alpha-burning (or “alpha-burner”) design has 202 μm of DT, 41 μm of CH, and an outer radius of 1487 μm . The ignition design has 191 μm of DT, 41 μm of CH, and an outer radius of 1482 μm . Each design uses a triple-picket pulse shape to shape the adiabat, and both designs achieve a high implosion speed of $\sim 400 \mu\text{m}/\text{ns}$, sufficient to generate high burn-averaged hot-spot pressures of $\sim 170 \text{ Gbar}$. Both designs have moderately low IFARs: the ignition design has an IFAR of 23 and a minimum end-of-pulse, density-weighted adiabat of 2.8, and the alpha burner has a somewhat lower IFAR of 21 with a larger ablator adiabat, resulting in an end-of-pulse, density-weighted adiabat of 4.6. Both of these IFARs are lower than that of a previous PDD-ignition design [9], which was shown to withstand the effects of laser imprint. (The simulations presented here include only perturbations related to port geometry, repointing, CBET, and nonlocal heat transport.) The peak areal density for the alpha burner is $1.4 \text{ g}/\text{cm}^2$, compared to $1.7 \text{ g}/\text{cm}^2$ for the ignition design.

The primary difference between these two designs is shown in the peak-convergence ion temperature and density plots of figure 2; the alpha-burning design, which uses the tricolor configuration, suffers from a larger north–south asymmetry, resulting in a south polar spike penetrating the hot spot. This spike does not preclude ignition; in fact, by stopping alpha particles near the center of the hot spot, it aids in ignition for a low-adiabat–igniting version of this design. However, the spike has a deleterious effect on the target margin and the integrity of the hot spot. The balanced tricolor design has much-greater north–south symmetry and, as a result, a more-uniform hot spot, making it a more-robust design. The alpha-burning design achieves a total neutron yield of 1.2×10^{17} , and the igniting design achieves a gain of 41. While the alpha-burning design does not ignite, it operates at a high adiabat for acceleration-phase stability and the neutrons generated by bootstrap heating are over $3\times$ that generated by compression alone.

4. Conclusions

Ample experimental and theoretical evidence exists to suggest that both CBET and nonlocal electron transport are necessary for modeling PDD on the NIF; whereas for spherical direct drive, a time-varying flux limiter might suffice to mimic these effects. In PDD, the deposition and heat transport have a strong dependence on the polar angle. We have presented here models of 1.8-MJ PDD designs that incorporate these effects. The first design operates at a high adiabat to ensure acceleration-phase stability; it is predicted to generate $\sim 10^{17}$ neutrons. The second design generates high gain (41), while maintaining an IFAR of 23, suggesting good stability with respect to short-wavelength modes.

Acknowledgment

This material is based upon work supported by the Department of Energy National Nuclear Security Administration under Award Number DE-NA0001944, the University of Rochester, and the New York State Energy Research and Development Authority. The support of DOE does not constitute an endorsement by DOE of the views expressed in this abstract.

References

- [1] Paisner J, Boyes J D, Kumpan S A, *et al.* 1994 *Laser Focus World* **30** 75
- [2] Skupsky S, Marozas J A, Craxton R S, *et al.* 2004 *Phys. Plasmas* **11** 2763
- [3] Marozas J A, Marshall F J, Craxton R S, *et al.* 2006 *Phys. Plasmas* **13** 056311
- [4] Murphy T J, Krasheninnikova N S, Kyrala G A, S *et al.* 2015 *Phys. Plasmas* **22** 092707
- [5] Cao D, Moses G, Delettrez J 2015, *Phys. Plasmas* **22** 082308
- [6] Marozas J A, Collins T J B, Zuegel J D, Radha P B, Marshall F J and Seka W 8–13 June 2014 presented at the 44th Annual Anomalous Absorption Conference Estes Park CO
- [7] Randall C J, Albritton J R, Thomson J J 1981 *Phys. Fluids* **24** 1474
- [8] Goncharov V N, Gotchev O V, Vianello E, *et al.* 2006 *Phys. Plasmas* **13** 012702
- [9] Collins T J B, Marozas J A, Anderson K S, *et al.* 2012 *Phys. Plasmas* **19** 05630